

Stress evolution following the 1811–1812 large earthquakes in the New Madrid Seismic Zone

Qingsong Li, Mian Liu, and Eric Sandvol

Department of Geological Sciences, University of Missouri, Columbia, Missouri, USA

Received 1 December 2004; revised 29 April 2005; accepted 18 May 2005; published 15 June 2005.

[1] Following a series of large ($M_w = 7.0\text{--}7.5$) earthquakes in the New Madrid Seismic Zone (NMSZ) in the central US during 1811 and 1812, more than a dozen moderate-size ($M > 5$) earthquakes occurred in this region, but mostly outside of the NMSZ fault zone. We have simulated the evolution of Coulomb stress and strain energy in the NMSZ and surrounding regions following the large 1811–1812 events in a three-dimensional viscoelastic finite element model. The results show that much of the stress and strain energy released by the large 1811–1812 events has migrated to southern Illinois and eastern Arkansas, consistent with the seismicity distribution. This inherited strain energy in these areas is capable of producing damaging ($M = 6\text{--}7$) earthquakes today. **Citation:** Li, Q., M. Liu, and E. Sandvol (2005), Stress evolution following the 1811–1812 large earthquakes in the New Madrid Seismic Zone, *Geophys. Res. Lett.*, *32*, L11310, doi:10.1029/2004GL022133.

1. Introduction

[2] During the winter between 1811 and 1812, at least three large earthquakes ($M_w = 7.0\text{--}7.5$) [Hough *et al.*, 2000] occurred in the New Madrid Seismic Zone (NMSZ), which is delineated by instrumental seismicity in Figure 1. Each of these main shocks was followed by numerous large aftershocks ($M > 6.0$) [Johnston and Schweig, 1996]. The main NMSZ faults include the southwestern segments (the Blytheville arch and the Blytheville Fault Zone), the NW trending Reelfoot Fault, and the northeastern segment (the New Madrid North Fault) (Figure 1). Only the Reelfoot Fault is exposed to the surface, other segments are delineated by seismicity, reflection and aeromagnetic data [Hildenbrand and Hendricks, 1995; Johnston and Schweig, 1996]. These faults are believed to be within a failed rift system formed in Late Proterozoic to Early Cambrian times [Ervin and McGinnis, 1975]. We hereinafter use NMSZ fault zones when referring to these fault structures.

[3] The cause of seismicity in the NMSZ is not well understood [Johnston and Schweig, 1996]. Paleoseismological data indicate two major events, around AD 900 and AD 1450, in the NMSZ comparable to the large 1811–1812 earthquakes [Tuttle and Schweig, 1995; Tuttle *et al.*, 2002]. These data imply a recurrence interval of ~ 500 years for large earthquakes in the NMSZ, at least in the past two thousand years [Tuttle *et al.*, 2002]. However, the GPS data

show insignificant strain rates around the NMSZ [Newman *et al.*, 1999], inconsistent with the conclusions drawn from the paleoseismic data. Some workers attempted to seek solution in some kind of local loading presumably related to the rift structure in the lower crust [Kenner and Segall, 2000; Pollitz *et al.*, 2001], but these structures are poorly constrained.

[4] Among the uncertainties of the NMSZ seismicity one fact stands solid – some large earthquakes occurred here in 1811–1812. In this study we choose to focus on the potential impact of the 1811–1812 large events on seismicity within the NMSZ and surrounding regions in the following two centuries. Although thousands of micro-earthquakes ($M < 4$) have been recorded within the NMSZ in the past decades, most of the major earthquakes ($M > 5$) in this region since 1812 occurred not within the NMSZ fault zone but in the surrounding areas (Figure 1). This raises the question of where the next large earthquake in the central United States would most likely occur.

2. Model

[5] We address this question by simulating the evolution of the Coulomb stress following the 1811–1812 events. Earthquake-induced changes of Coulomb stress have been shown to be useful in predicting spatial patterns of seismicity in plate boundary zones [King *et al.*, 1994; Stein *et al.*, 1992; Zeng, 2001], but how these processes work in intraplate settings has not been fully explored. We constructed a three-dimensional finite element model that spans a $556\text{ km} \times 556\text{ km}$ area centered on the NMSZ (Figure 1). The model crust is 40 km thick with a viscoelastic rheology. The stiff upper 20 km is assumed to be elastic for deformation over the timescale of hundreds of years. Viscosities between 10^{19} and 10^{21} Pa s, likely the limits for the NMSZ lower crust [Kenner and Segall, 2000], were tested in the model. The Young's modulus and the Poisson's ratio are taken to be 8.75×10^{10} Pa and 0.25, respectively, for the entire crust [Turcotte and Schubert, 1982].

[6] The compressive stresses across the North American plate were simulated by applying a 0.5 mm/yr velocity boundary condition on the eastern and western edges of the model (Figure 1). This produces a strain rate of $\sim 2 \times 10^{-9}$ /yr over the model domain, which is likely the upper bound of internal deformation rate within the North American plate based on GPS and seismological data [Anderson, 1986; Newman *et al.*, 1999; Zoback *et al.*, 2002]. The NMSZ fault zones are simplified in the model with two vertical strike-slip branches connected by the NW-trending reverse fault dipping 45° southwest, based on inferred fault geometry [Chiu *et al.*, 1992; Mueller and

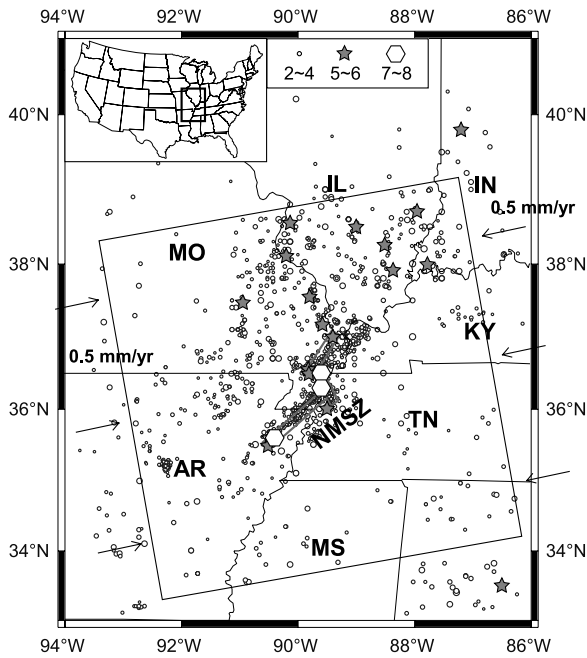


Figure 1. Earthquake epicenters in the NMSZ and surrounding regions (the location is shown in the inset). Modern earthquake data ($M > 2$ since 1974, circles) are from the NEIC and CERI Catalog (1974–2003); pre-1974 and historic earthquake data ($M > 5$, stars) are from Stover and Coffman [Stover and Coffman, 1993]. Hexagons show the large 1811–1812 events [Stover and Coffman, 1993]. The NMSZ is delineated by solid lines. The frame and arrows show the model domain and boundary conditions.

Pujol, 2001]. The faults were simulated by special fault elements within which plastic deformation is used to simulate stress drop and displacement during earthquakes. The initial stress state just before the 1811–1812 large earthquakes was unknown; we assume it to be everywhere close to the yield strength of the upper crust [Townend and Zoback, 2000; Zoback et al., 2002], which is consistent

with the widespread seismicity in the NMSZ and surrounding regions.

3. Results

[7] To focus on stress evolution following the large 1811–1812 earthquakes, we simulated these three events, spanning over three months, as having occurred simultaneously. This was done with ~ 5 m instant slip along the model NMSZ fault zone, resulting in a Coulomb stress drop of 5 MPa within the fault zone, as estimated by Hough et al. [2000]. The Coulomb stress on a plane is defined as $\sigma_f = \tau_\beta - \mu\sigma_\beta$, where τ_β is the shear stress on the plane, σ_β is the normal stress, and μ is the effective coefficient of friction [King et al., 1994]. For regions outside the NMSZ fault zones where seismogenic faults are not well defined, we calculate the optimal Coulomb stress, which is the stress on planes optimally orientated for failure [King et al., 1994].

[8] Figure 2a shows stress migration immediately following the 1811–1812 events. In the upper crust the maximum stress increases are near the NE and SW ends of the NMSZ. Conversely, stress decreases within the NMSZ fault zones and much of the surrounding areas. Some of the stress migrated to the lower crust under the fault zone, but postseismic viscous relaxation in the ductile lower crust then caused stress to gradually re-accumulate in the upper crust, mainly in the fault zone and in the quadrants of increased coseismic Coulomb stress, similar to previous viscoelastic model results [Freed and Lin, 2001; Rydelek and Pollitz, 1994]. Although far-field tectonic loading tends to increase stress in the whole region, the rate is slow. Two hundred years after the 1811–1812 large earthquakes, the NMSZ remains in a stress shadow where stress has not reached pre-1811–1812 values. The largest Coulomb stress increases are in southern Illinois and eastern Arkansas, where most of the major earthquakes since 1812 have occurred (Figure 2).

[9] The aftershocks of the 1811–1812 large events were not included in the calculation for lack of constraints, but their effects are likely minor in terms of energy release. This can be seen from Figure 2b where the impact of the two largest earthquakes in the NMSZ region since 1812, the

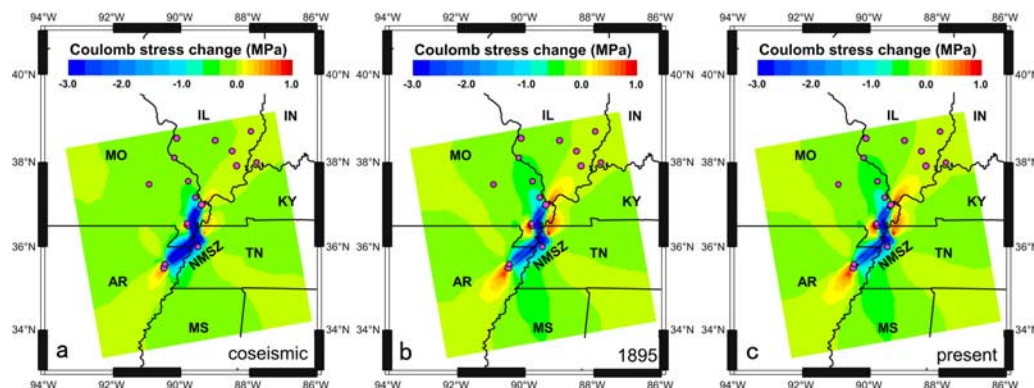


Figure 2. (a) Predicted coseismic Coulomb stress change during the 1811–1812 earthquakes in the NMSZ. (b) Predicted Coulomb stress change after the 1843 Marked Tree, Arkansas, and the 1895 Charleston, Missouri, earthquakes. (c) Predicted Coulomb stress change at present. The red dots are the major earthquakes ($M > 5$) since 1812 [Stover and Coffman, 1993].

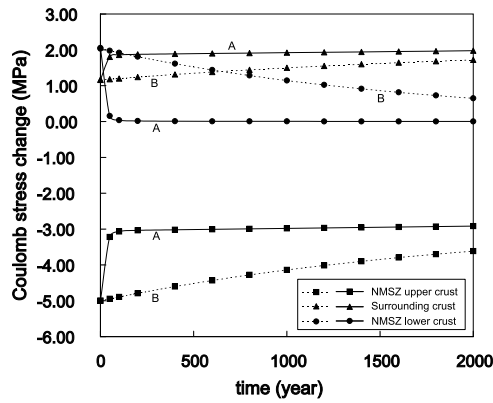


Figure 3. The calculated evolution of the Coulomb stress since the 1811–1812 large earthquakes. The dashed lines are for case B with a higher viscosity (1.0×10^{21} Pa s) for the lower crust, and the solid lines are for case A with a lower viscosity (1.0×10^{19} Pa s) for the lower crust. The stress evolution in the upper crust outside of the NMSZ (surrounding crust) is for the quadrants of increasing Coulomb stress (see Figure 2).

1895 Charleston, Missouri earthquake ($M = 6.2$) and the 1843 Marked Tree, Arkansas earthquake ($M = 6.0$), was calculated. The results show some local stress changes near the epicenters of these events, but the general stress pattern remains dominated by the 1811–1812 large events. The present Coulomb stress field calculated with these two events (Figure 2c) is similar to that calculated without them. We also found that, although these two events consumed some of the strain energy released by the 1811–1812 large events, their impact on the total strain energy budget is minor (see below). Note that the results in Figure 2 were obtained by assuming a complete healing of the NMSZ faults, such that the yield strength returned to the pre-1811–1812 level immediately following the large events. If the NMSZ faults were unhealed or partially healed, stress reaccumulation within the NMSZ fault zone would be even slower.

[10] The postseismic stress change owing to viscous relaxation is dependent on the viscosity of the lower crust and perhaps the lithospheric mantle [Freed and Lin, 2001].

Figure 3 shows the predicted stress evolution within the NMSZ and in the ambient regions of increasing Coulomb stresses for two end-member lower crust viscosity values. In both cases postseismic viscous relaxation reduces stress in the lower crust and increases stress in the upper crust; the process is faster when the lower crustal viscosity is lower. However, in either case stress rebuilding within the NMSZ fault zone lags behind that in the ambient crust including southern Illinois and eastern Arkansas.

[11] Figure 4a shows the calculated seismic energy release based on historic and modern earthquake data from the National Earthquake Information Center (NEIC) catalog (<http://neic.usgs.gov/neis/epic/epic.html>). We used the Gutenberg-Richter's formula [Lay and Wallace, 1995], and approximated all magnitudes as M_s . The spatial pattern is dominated by a dozen moderate-size events ($M > 5$) since 1812, especially the two $M \sim 6$ events near the NE and SW tips of the NMSZ (Figure 2b). The released seismic energy may be compared with the change of strain energy, which is associated with the stress migration following the 1811–1812 large earthquakes. Figure 4b shows the excess strain energy, calculated by assigning a strain change in each element, if needed, to bring the deviatoric stress below the yield strength of the crust during a time step. The total excess strain energy accumulation over a single time step at a given place is given by a vertical integration of the product of stress and the strain change. The spatial pattern of the calculated excess strain energy is consistent with the seismic energy release in the past two centuries (Figure 4a), but the magnitude is two to three orders higher presumably because not all energy has been released via earthquakes. The relation between strain energy before the large earthquakes, the energy released during them, and the fraction of energy radiated as seismic waves remains unclear [Kanamori, 1978]. Assuming only $\sim 10\%$ of the energy was radiated as seismic waves [Lockner and Okubo, 1983], we can multiply the estimated seismic energy release (Figure 4a) by 10 to get an estimate of total energy released by earthquakes in the past two centuries. Subtracting it from the excess strain energy in Figure 4b gives the residual strain energy, some of it may be released by future earthquakes. The partition between seismic and aseismic energy is uncertain [Ward, 1998]. Figure 4c shows the available seismic energy if only 2.5% of the total

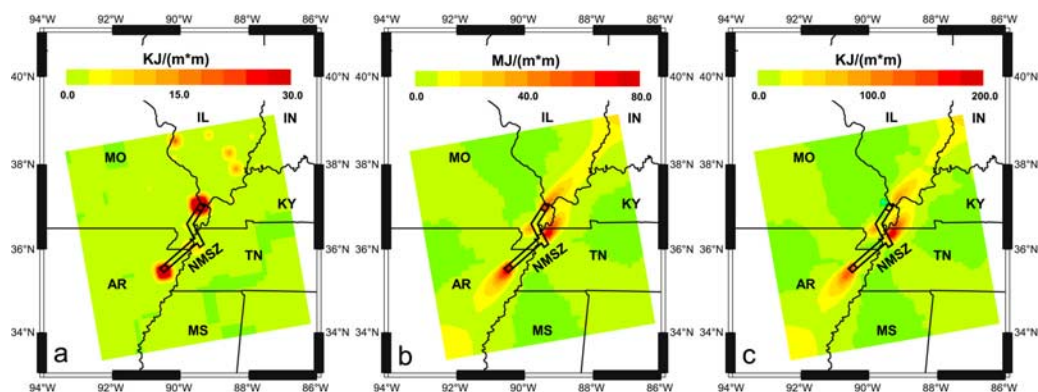


Figure 4. (a) Estimated seismic energy release in the NMSZ and surrounding regions since 1812. (b) Predicted total excess strain energy since the 1811–1812 events. (c) Predicted seismic strain energy in the crust today available for producing earthquakes.

excess strain energy will be released in future earthquakes. This energy is still capable to produce a number of $M = 6-7$ earthquakes in southern Illinois and eastern Arkansas today.

4. Discussion and Conclusions

[12] We have shown that some of the strain energy released during the 1811–1812 earthquakes may have migrated to the ambient crust and perhaps caused, or at least triggered, the moderate-size earthquakes in regions surrounding the NMSZ. The calculated build up of Coulomb stress and strain energy from the 1811–1812 events is high enough to produce some damaging earthquakes today in southern Illinois and eastern Arkansas. Similar conclusions have been reached from studies of recently instrumentally recorded aftershocks [Gomberg, 1993; Mueller et al., 2004].

[13] The prediction of the NMSZ fault zone remaining in a stress shadow two hundred years after the 1811–1812 large earthquakes is hardly surprising, given the stability of the North American plate interior [Dixon et al., 1996; Gan and Prescott, 2001]. The $<2 \times 10^{-9}$ /yr strain rate within the stable North America [Gan and Prescott, 2001] implies a <0.02 MPa far-field secular loading since 1812, much less than the stress released by the 1811–1812 earthquakes (~ 5 MPa). This is significantly different from earthquakes in plate boundary zones where the accumulated strain energy is dominated by tectonic loading. To reconcile with the paleoseismic evidence of ~ 500 years recurrence interval for large earthquakes in the NMSZ, some mechanisms of local loading is required. These mechanisms include sinking of a mafic body within the Reelfoot rift [Pollitz et al., 2001] and a sudden thermal event that weakens the NMSZ lithosphere [Kenner and Segall, 2000]. Further testing of these mechanisms needs a more refined image of lower crustal and mantle lithospheric structures than those currently available. A local loading under the NMSZ would enhance the strain energy in the ambient crust predicted in this study.

[14] **Acknowledgments.** This work was supported by U.S. Geological Survey grant No. 04HQGR0046. We thank Seth Stein and Jian Lin for helpful comments, and the GRL referees, Jerome van der Woerd and Mike Ellis for constructive review.

References

- Anderson, J. G. (1986), Seismic strain rates in the central and eastern United States, *Seismol. Soc. Am. Bull.*, *76*, 273–290.
- Chiu, J. M., A. C. Johnston, and Y. T. Yang (1992), Imaging the active faults of the central New Madrid Seismic Zone using PANDA array data, *Seismol. Res. Lett.*, *63*, 375–393.
- Dixon, T. H., A. Mao, and S. Stein (1996), How rigid is the stable interior of the North American plate?, *Geophys. Res. Lett.*, *23*, 3035–3038.
- Ervin, C. P., and L. D. McGinnis (1975), Reelfoot Rift: Reactivated precursor to the Mississippi Embayment, *Geol. Soc. Am. Bull.*, *86*, 1287–1295.
- Freed, A. M., and J. Lin (2001), Delayed triggering of the 1999 Hector Mine earthquake by viscoelastic stress transfer, *Nature*, *411*, 180–183.
- Gan, W., and W. H. Prescott (2001), Crustal deformation rates in central and eastern U.S. inferred from GPS, *Geophys. Res. Lett.*, *28*, 3733–3736.
- Gomberg, J. S. (1993), Tectonic deformation in the New Madrid seismic zone; inferences from map view and cross-sectional boundary element models, *J. Geophys. Res.*, *98*, 6639–6664.
- Hildenbrand, T. G., and J. D. Hendricks (1995), Geophysical setting of the Reelfoot Rift and relations between rift structures and the New Madrid seismic zone, *U.S. Geol. Surv. Prof. Pap.*, *1538-E*, 1–30.
- Hough, S. E., J. G. Armbruster, L. Seeber, and J. F. Hough (2000), On the modified Mercalli intensities and magnitudes of the 1811–1812 New Madrid earthquakes, *J. Geophys. Res.*, *105*, 23,839–23,864.
- Johnston, A. C., and E. S. Schweig (1996), The enigma of the New Madrid earthquakes of 1811–1812, *Annu. Rev. Earth Planet. Sci.*, *24*, 339–394.
- Kanamori, H. (1978), Quantification of earthquakes, *Nature*, *271*, 411–414.
- Kenner, S. J., and P. Segall (2000), A mechanical model for intraplate earthquakes: Application to the New Madrid Seismic Zone, *Science*, *289*, 2329–2332.
- King, G. C. P., R. S. Stein, and J. Lin (1994), Static stress changes and the triggering of earthquakes, *Bull. Seismol. Soc. Am.*, *84*, 935–953.
- Lay, T., and T. C. Wallace (1995), *Modern Global Seismology*, 383–385 pp., Elsevier, New York.
- Lockner, D. A., and P. G. Okubo (1983), Measurements of frictional heating in granite, *J. Geophys. Res.*, *88*, 4313–4320.
- Mueller, K., and J. Pujol (2001), Three-dimensional geometry of the Reelfoot blind thrust: Implications for moment release and earthquake magnitude in the New Madrid Seismic Zone, *Bull. Seismol. Soc. Am.*, *91*, 1563–1573.
- Mueller, K., S. E. Hough, and R. Bilham (2004), Analysing the 1811–1812 New Madrid earthquakes with recent instrumentally recorded aftershocks, *Nature*, *429*, 284–288.
- Newman, A., S. Stein, J. Weber, J. Engeln, A. Mao, and T. Dixon (1999), Slow deformation and lower seismic hazard at the New Madrid Seismic Zone, *Science*, *284*, 619–621.
- Pollitz, F. F., L. Kellogg, and R. Buergermann (2001), Sinking mafic body in a reactivated lower crust: A mechanism for stress concentration at the New Madrid Seismic Zone, *Bull. Seismol. Soc. Am.*, *91*, 1882–1897.
- Rydelek, P. A., and F. F. Pollitz (1994), Fossil strain from the 1811–1812 New Madrid earthquakes, *Geophys. Res. Lett.*, *21*, 2303–2306.
- Stein, R. S., G. C. King, and J. Lin (1992), Change in failure stress on the southern San Andreas Fault system caused by the 1992 magnitude = 7.4 Landers earthquake, *Science*, *258*, 1328–1332.
- Stover, C. W., and J. L. Coffman (1993), Seismicity of the United States, 1568–1989 (revised), *U.S. Geol. Surv. Prof. Pap.*, *1527*, 418 pp.
- Townend, J., and M. D. Zoback (2000), How faulting keeps the crust strong, *Geology*, *28*, 399–402.
- Turcotte, D. L., and G. Schubert (1982), *Geodynamics: Applications of Continuum Physics to Geological Problems*, 450 pp., John Wiley, Hoboken, N. J.
- Tuttle, M. P., and E. S. Schweig (1995), Archeological and pedological evidence for large prehistoric earthquakes in the New Madrid Seismic Zone, central United States, *Geology*, *23*, 253–256.
- Tuttle, M. P., E. S. Schweig, J. D. Sims, R. H. Lafferty, L. W. Wolf, and M. L. Haynes (2002), The earthquake potential of the New Madrid Seismic Zone, *Bull. Seismol. Soc. Am.*, *92*, 2080–2089.
- Ward, S. N. (1998), On the consistency of earthquake moment rates, geological fault data, and space geodetic strain: The United States, *Geophys. J. Int.*, *134*, 172–186.
- Zeng, Y. (2001), Viscoelastic stress-triggering of the 1999 Hector Mine earthquake by the 1992 Landers earthquake, *Geophys. Res. Lett.*, *28*, 3007–3010.
- Zoback, M. D., J. Townend, and B. Grollmund (2002), Steady-state failure equilibrium and deformation of intraplate lithosphere, *Int. Geology Rev.*, *44*(5), 383–401.

Q. Li, M. Liu, and E. Sandvol, Department of Geological Sciences, University of Missouri, Columbia, MO 65211, USA. (lium@missouri.edu)